Current Biology, Vol. 13, 828–832, May 13, 2003, ©2003 Elsevier Science Ltd. All rights reserved. DOI 10.1016/S0960-9822(03)00291-4

Flamingo Regulates R8 Axon-Axon and Axon-Target Interactions in the *Drosophila* Visual System

Kirsten-André Senti,[1,5,6] Tadao Usui,[3,5] Karin Boucke,[4] Urs Greber,[4] Tadashi Uemura,[3] and Barry J. Dickson[1,2,*]
[1]Research Institute of Molecular Pathology (IMP)
[2]Institute of Molecular Biotechnology of the Austrian Academy of Sciences (IMBA)
Dr. Bohr-Gasse 7
A-1030 Vienna
Austria
[3]Laboratory of Molecular Genetics
Institute for Virus Research
Kyoto University
Sakyo-ku
Kyoto 606-8507
Japan
[4]Zoologisches Institut
Universität Zürich
Winterthurerstrasse 190
CH-8057 Zürich
Switzerland

Summary

Photoreceptors (R cells) in the *Drosophila* retina connect to targets in three distinct layers of the optic lobe of the brain: R1–R6 connect to the lamina, and R7 and R8 connect to distinct layers in the medulla [1]. In each of these layers, R axon termini are arranged in evenly spaced topographic arrays. In a genetic screen for mutants with abnormal R cell connectivity, we recovered mutations in *flamingo* (*fmi*). *fmi* encodes a seven-transmembrane cadherin, previously shown to function in planar cell polarity [2] and in dendritic patterning [3]. Here, we show that *fmi* has two specific functions in R8 axon targeting: it facilitates competitive interactions between adjacent R8 axons to ensure their correct spacing, and it promotes the formation of stable connections between R8 axons and their target cells in the medulla. The former suggests a general role for Fmi in establishing nonoverlapping dendritic and axonal target fields. The latter, together with the finding that N-Cadherin has an analogous role in R7 axon-target interactions [4], points to a cadherin-based system for target layer specificity in the *Drosophila* visual system [1].

Results and Discussion

Flamingo Is Required Autonomously for Photoreceptor Axon Targeting

We recovered nine alleles of *fmi* in a genetic screen for mutations disrupting photoreceptor (R cell) connectivity in the *Drosophila* visual system [5]. In this screen, and in most of the analyses reported here, photoreceptor axon projections were examined in whole-eye mosaics generated with *eyFLP* [5]. In wild-type animals and control mosaics, photoreceptor axons terminate in smooth topographic arrays in three distinct layers of the optic lobe: R1–R6 terminate in the lamina, R7 terminates in the M6 layer of the medulla, and R8 terminates in the more superficial M3 layer (Figure 1A). In contrast, R axons in *fmi* mosaics terminate in a highly disorganized pattern, particularly within the medulla (Figure 1B). These defects were rescued by restoring *fmi* function specifically in the eye by using a *GMR-fmi* transgene (Figure 1C). This confirms that *fmi* function is required autonomously in the eye for correct R axon targeting. Importantly, this *GMR-fmi* transgene does not produce any dominant guidance or targeting defects, indicating that *fmi*'s function does not require its restricted expression in just a subset of photoreceptor cells.

Since *fmi* is also required for correct ommatidial polarity in the eye [6–8], we wondered whether these axon targeting defects might be secondary to polarity defects. To test this, we examined R axon projections in animals mutant for *frizzled*, *dishevelled*, *strabismus*/*Van Gogh*, and *prickle-spiny legs*, genes that act together with *fmi* in the establishment of ommatidial polarity [9]. For all of these mutants, R axon projection patterns appeared normal, despite the defects in ommatidial polarity (data not shown, but see also [10]). We conclude that ommatidial polarity defects do not necessarily cause strong axon targeting defects, and that the function of *fmi* in axon targeting is mediated by a pathway distinct from that used in establishing ommatidial polarity.

Flamingo Is Required for Layer-Specific Targeting of R8 Axons

For a more detailed analysis of photoreceptor axon targeting in *fmi* mosaics, we used markers specific for each subclass of photoreceptors: *Rh1-τlacZ* for R1–R6, *Rh4-τlacZ* to label ~70% of R7 cells, and *Rh6-GAL4 UAS-τlacZ* to label ~70% of R8 cells. These markers revealed a highly specific R8 targeting defect (Figures 2C and 2G). In contrast, R1–R6 axons correctly target the lamina (Figures 2A and 2E), and R7 axons generally appear to select their correct target layer in the medulla, although their termini are slightly disorganized (Figures 2B and 2F).

Since the R7 axon from each ommatidium extends into the medulla some 12 hr after the R8 axon, we wondered if the mild R7 targeting defects might merely be secondary to the severe defects in R8 targeting. To test for a specific role of *fmi* in R7 targeting, we used *GMR-FLP* and the MARCM system to generate and label single mutant R7 cells in an otherwise heterozygous animal [4, 11]. The axons of these *fmi* mutant R7 cells always targeted the correct layer in the medulla (n = 102 in five optic lobes; Figures 2D and 2H).

*Correspondence: dickson@nt.imp.univie.ac.at (B.J.D.); tuemura@virus.kyoto-u.ac.jp (T.U.)
[5]These authors contributed equally to this work.
[6]Present address: Karolinska Institute, Department of Molecular and Cell Biology, Brezeliusväg 35, S-17177 Stockholm, Sweden.

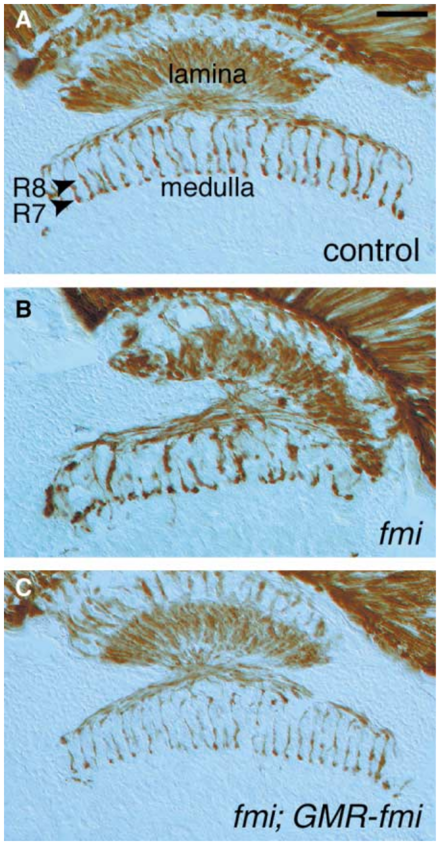

Figure 1. Flamingo Is Required Autonomously for Retinal Axon Targeting

(A–C) Horizontal head sections of (A) control mosaics, (B) *fmi*^{E59} mosaics, and (C) *fmi*^{E59} mosaics rescued with a *GMR-fmi* transgene. Whole-eye clones were generated with *eyFLP*, and R axons were visualized by using a *glass-lacZ* marker and anti-β-galactosidase staining. The arrowheads in (A) indicate layers of R8 and R7 termini in the medulla. Anterior is oriented toward the upper left. The scale bar represents 25 μm.

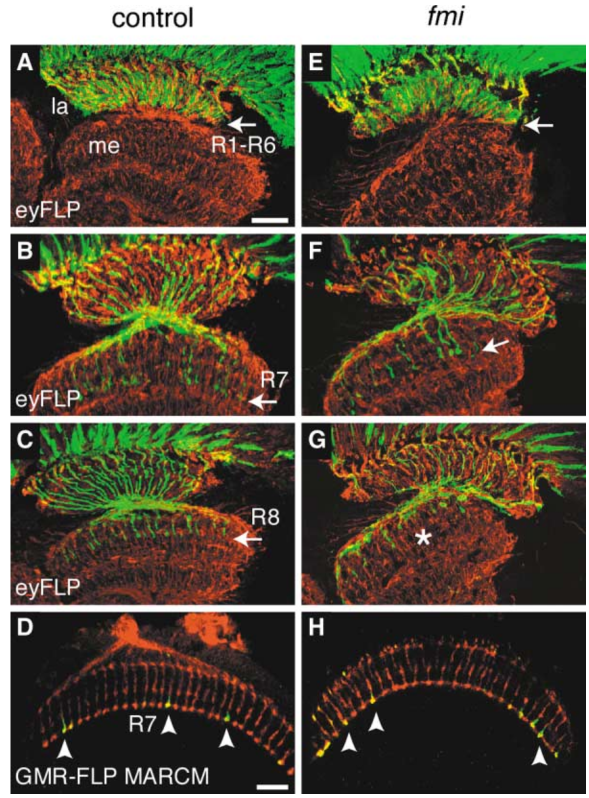

Figure 2. Flamingo Is Required for R8 Target Layer Specificity

(A–H) Horizontal head sections of (A–D) control mosaics and (E–H) *fmi*^{E59} mosaics generated by using either (A–C, E–G) *eyFLP* to make whole-eye mosaics or (D and H) *GMR-FLP* and MARCM to generate single mutant R7 cells. Specific axonal markers (green) were visualized with (A–C, E–G) anti-β-galactosidase or (D and H) anti-GFP. Counterstaining (red) was performed with either (A–C, E–G) mAb 22C10 to label all neurons or (D and H) mAb 24B10 to label all photoreceptor axons. (E–G) Note also the slight misalignment of the medulla (me) with respect to the retina and lamina (la) in *fmi* mosaics. This defect is commonly observed in photoreceptor connectivity mutants and can usually be rescued by eye-specific expression, as is the case for *fmi* (Figure 1C). It reflects a failure of the medulla to complete its normal 90° rotation during late pupal development. (A and E) R1–R6 axons, labeled with *Rh1-τlacZ*, terminate in the lamina (arrow) in both control and *fmi* mosaics. (B and F) R7 axons, labeled with *Rh4-τlacZ*, terminate in a deep layer of the medulla (arrow), and only very mild defects are observed in *fmi* mosaics. (C and G) R8 axons, labeled with *Rh6-GAL4 UAS-τlacZ*, terminate in a single layer of the medulla in control animals ([C], arrow) but are highly disorganized and often terminate at superficial levels in *fmi* mosaics ([G], asterisk). (D and H) Single mutant R7 axons, generated with *GMR-FLP* and MARCM and labeled with *A181-GAL4 UAS-synaptobrevin-GFP*, terminate in the correct layer in both control and *fmi* mosaics (arrowheads). The scale bars represent 25 μm.

From this analysis, we conclude that *fmi* is required in the eye for R8 axons to select targets in the correct layer of the medulla, but not for the target layer specificity of R1–R6 or R7. This precludes neither an additional nonautonomous requirement for *fmi* within the target region nor a role for *fmi* in any R cell for the selection of the appropriate synaptic partners within the target layer.

Flamingo Is Required for the Correct Spacing and Morphology of R8 Growth Cones

R8 axons first extend from the eye imaginal disc into the optic lobe during the third instar larval stage. The *Rh6* marker is not expressed at this stage, and so to follow the initial projections of the R8 axons, we generated an early R8 marker *ato-τmyc* (see the Experimental Procedures). With this marker, it appeared that most if not all R8 axons do initially reach their correct target layer in the medulla (Figure 3F). Since many R8 axons terminate in more superficial layers in the adult (Figure 2G), we infer that these R8 axons fail to form stable contacts in their target region and subsequently retract to more superficial layers.

In wild-type animals, R8 axons form evenly spaced topographic arrays in the medulla, with "inverted-Y-shaped" growth cones (Figures 3A and 3B). In *fmi* mosaics, the R8 growth cones are irregularly spaced and have a more "club-like" morphology, but they have many

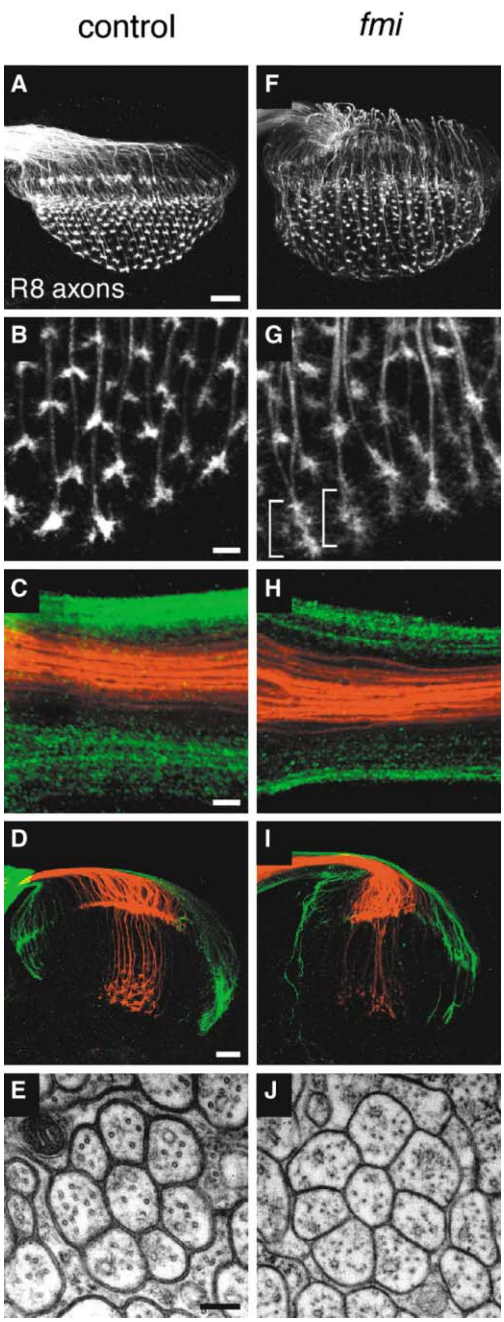

Figure 3. Morphology, Spacing, Topography, and Fasciculation of Photoreceptor Axons

(A–J) (A–D, F–I) Whole mount eye-brain complexes of third instar larvae and (E and J) optic stalk cross-sections of white prepupae from (A–E) control and (F–J) *fmi*^{E59} mosaics generated with *eyFLP*. (A, B, F, and G) (A and F) Low- and (B and G) high-magnification views of optic lobes. R8 axons are labeled with *ato-τmyc*. The brackets in (G) indicate examples of overlapping R8 growth cones. (C, H, D, and I) (C and H) A high-magnification view of the optic stalk and (D and I) a low-magnification view of the optic lobe of animals carrying the *omb-τlacZ* marker for polar axons (green) and the *sema2b-τmyc* marker for equatorial axons (red). (E and J) Transmission electron micrographs of uranylacetate-contrasted ultrathin sections through the optic stalk. The scale bars represent 20 μm in (A) and (D), 2 μm in (B) and (C), and 0.2 μm in (E).

elaborate fine processes (Figures 3F and 3G). The processes of individual R8 growth cones often overlap extensively, something we only rarely observe in control animals (Figures 3B and 3G; see also [12]).

Despite this irregular spacing, the entire target field appears to be filled, and there does not appear to be any dramatic misrouting of axons within the optic lobe. This suggests that the overall topographic order is largely preserved in *fmi* mosaics. We confirmed this for the dorsoventral axis by using markers specific for polar (i.e., dorsal- and ventral-most) axons (*omb-τlacZ*; [13]) and equatorial axons (*Sema2b-τmyc*; [14]). In *fmi* mosaics, as in control mosaics, these axons maintain their correct topographic positions as they extend within the eye disc (not shown), through the optic stalk (Figures 3C and 3H), and into the optic lobe (Figures 3D and 3I). We lack analogous markers to assess topographic mapping along the anterior-posterior axis, but the ordered posterior-to-anterior filling of the medulla target field in all of the preparations we examined (e.g., Figure 3F) is strong evidence that, along this axis too, topographic order is preserved.

Since Fmi is a homophilic cell adhesion molecule [2], we wondered whether it might also contribute to the bundling of photoreceptor axons into their discrete ommatidial fascicles. We tested this by using electron microscopy to examine the composition and structure of ommatidial fascicles within the optic stalk. The only difference we noted in *fmi* compared to control mosaics was a slight (5.0%) increase in the number of fascicles comprising more than eight R axons ($n = 900$ and 587, respectively). This difference can be attributed to the low frequency of ommatidia containing extra R cells [8]. Otherwise, *fmi* mosaics were indistinguishable from the controls (Figures 3E and 3J), indicating that Fmi does not function in the formation of ommatidial fascicles.

Flamingo Is Expressed on Photoreceptor Axons and in the Target Region

We used anti-Fmi mAb 74 [2] to assess the distribution of Fmi protein in the developing visual system. At the third instar larval stage, Fmi protein is strongly expressed within the lamina plexus, where R1–R6 axons terminate, and in the R7/R8 termination region in the medulla (Figures 4A–4C). In photoreceptor axons, Fmi is highly localized to the growth cone; only very low levels of staining are seen along the axon shaft. Strong staining was also observed within the medulla and lobula. This staining appears to localize to the processes and termini, respectively, of medulla cortical neurons (as visualized with *Ap-GAL4* and *UAS-CD8-GFP*; Figure 4C). We could not detect any Fmi protein in glia in the retina, lamina, or medulla (as visualized with *UAS-CD8-GFP* and the glia-specific drivers *1.3C2-GAL4* [15] and *Mz97-GAL4* [16]). In whole-eye *fmi* mosaics, most Fmi staining is lost in the lamina plexus, while staining in the medulla is reduced but not eliminated (data not shown). This confirms that Fmi protein in the lamina is largely confined to R1–R6 growth cones, while, in the medulla, some but not all Fmi protein is localized to R7 and/or R8 growth cones.

Fmi immunoreactivity persists in the lamina and me-

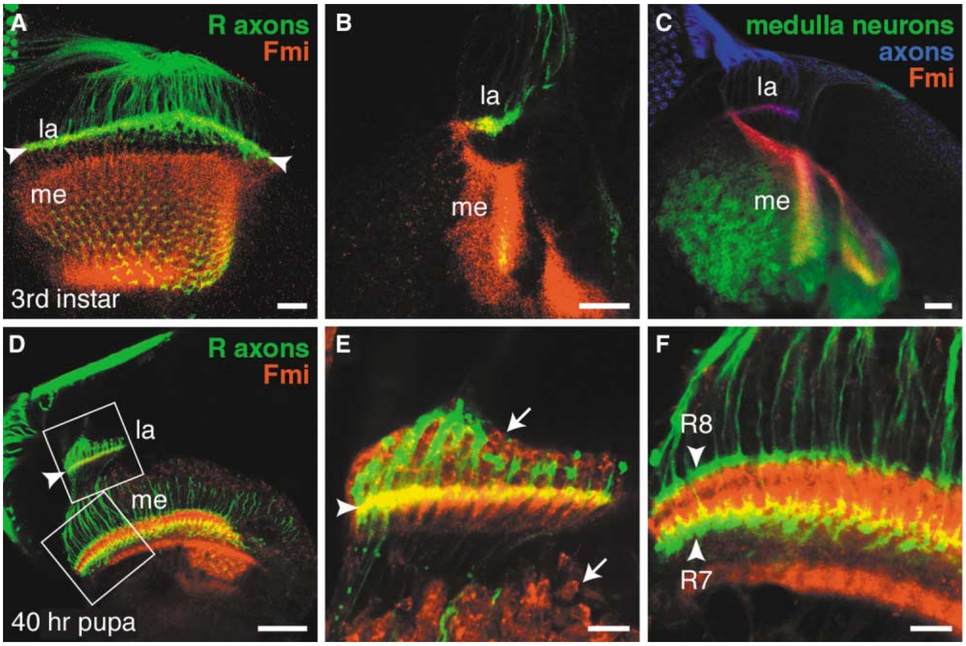

Figure 4. Flamingo Localizes to Photoreceptor Growth Cones and Specific Layers of the Developing Optic Lobes

(A–F) Wild-type (A–C) third instar larval and (D–F) 40-hr pupal eye-brain complexes stained with anti-Fmi (red). Photoreceptor axons were visualized with *glass-lacZ* (green in [A], [B], and [D]–[F]) or with anti-HRP (blue in [C]). In (C), medulla cortical neurons are visualized with *Ap-GAL4 UAS-CD8-GFP*. (B) and (C) are cross-sectional views; other panels are dorsal views. The arrowheads in (A), (D), and (E) indicate the lamina plexus; arrowheads in (F) indicate the layer of R8 and R7 termini. (E) and (F) are higher magnification views of the boxed regions shown in (D). The arrows in (E) indicate expression on lamina (upper) and medulla (lower) cortical neurons. la, lamina; me, medulla. The scale bars represent 20 μm in (A)–(C), 50 μm in (D), and 10 μm in (E) and (F).

dulla throughout early- and mid-pupal development, with increased staining of lamina and medulla cortical neurons (Figures 4D and 4E). By the mid-pupal stage, the R7 and R8 growth cones have become more widely separated (by ~10 μm), in part due to the intercalation of growth cones and processes from lamina and other neurons [1]. Intense Fmi staining is seen in the medulla neuropil in the region between the R8 and R7 termini, with only low levels in the layers immediately above the R8 termini or below the R7 termini (Figures 4D and 4F). Fmi also localizes to a single broad band deeper in the medulla and to the lobula.

Conclusions

Our results define two distinct and specific functions for Fmi in R axon targeting. First, it facilitates competitive or inhibitory interactions between adjacent R8 growth cones. Second, it promotes R8 axon-target interactions. These inhibitory interactions between R8 growth cones may be mechanistically related to those previously demonstrated for R7 axons [12]. Competitive interactions between retinal axons also contribute to the formation of an evenly spaced topographic map in the mammalian visual system [17, 18]. Mammalian Fmi proteins are also widely expressed in the developing nervous system [19–21] and thus are strong candidates to mediate similar competitive axon-axon interactions. This function of Fmi in R axons may also be analogous to its role in the dendritic tiling of the embryonic PNS, where competitive interactions involving Fmi prevent overlap between the dendritic fields of homologous sensory neurons [3].

In addition to this negative role in R8 axon-axon interactions, Fmi also appears to act positively in R8 axon-target interactions. Here, parallels can be drawn with the function of the classical cadherin, N-Cadherin, in R7 targeting. In both cases, mutant axons initially contact their correct medulla target layer, but then a specific subclass retracts: R7 retracts in the case of *N-Cadherin* [1, 4] and R8 retracts in the case of *fmi*. Distinct cadherins thus regulate distinct targeting decisions in the medulla and possibly act in this case as homophilic cell adhesion molecules. However, since both N-Cadherin and Fmi are expressed on all photoreceptor axons and in multiple layers in the optic lobe, these two cadherins alone cannot account for the distinct target layer selections of R7 and R8. Additional determinants must exist. One of these is the receptor tyrosine phosphatase LAR, which is specifically required for R7 target layer selection and may act by modulating N-Cadherin-mediated adhesion [22, 23]. Other factors are likely to emerge from ongoing genetic screens for layer-specific axon targeting in the *Drosophila* visual system [5, 22, 23].

Supplemental Data

Supplemental Data including the Experimental Procedures are available at http://images.cellpress.com/supmat/supmatin.htm.

Acknowledgments

We thank K. Paiha for assistance with confocal microscopy and C. Klämbt, I. Salecker, Y. Sun, and J. Thomas for reagents. This work was supported by funding from the Human Frontiers of Science Program (to B.J.D. and T.U.); the Austrian National Science Foundation and Boehringer Ingelheim GmbH (B.J.D.); and Core Research for Evolutional Science and Technology, the Japan Science and Technology Corporation, and the Brain Science Foundation (T.U.). K.-A.S. was supported in part by a fellowship from Boehringer Ingelheim Fonds.

Received: January 14, 2003
Revised: March 7, 2003
Accepted: March 17, 2003
Published: May 13, 2003

References

1. Clandinin, T.R., and Zipursky, S.L. (2002). Making connections in the fly visual system. Neuron *35*, 827–841.
2. Usui, T., Shima, Y., Shimada, Y., Hirano, S., Burgess, R.W., Schwarz, T.L., Takeichi, M., and Uemura, T. (1999). Flamingo, a seven-pass transmembrane cadherin, regulates planar cell polarity under the control of Frizzled. Cell *98*, 585–595.
3. Gao, F.B., Kohwi, M., Brenman, J.E., Jan, L.Y., and Jan, Y.N. (2000). Control of dendritic field formation in *Drosophila*: the roles of flamingo and competition between homologous neurons. Neuron *28*, 91–101.
4. Lee, C.H., Herman, T., Clandinin, T.R., Lee, R., and Zipursky, S.L. (2001). N-cadherin regulates target specificity in the *Drosophila* visual system. Neuron *30*, 437–450.
5. Newsome, T.P., Asling, B., and Dickson, B.J. (2000). Analysis of *Drosophila* photoreceptor axon guidance in eye-specific mosaics. Development *127*, 851–860.
6. Chae, J., Kim, M.J., Goo, J.H., Collier, S., Gubb, D., Charlton, J., Adler, P.N., and Park, W.J. (1999). The *Drosophila* tissue polarity gene *starry night* encodes a member of the protocadherin family. Development *126*, 5421–5429.
7. Yang, C.H., Axelrod, J.D., and Simon, M.A. (2002). Regulation of Frizzled by fat-like cadherins during planar polarity signaling in the *Drosophila* compound eye. Cell *108*, 675–688.
8. Das, G., Reynolds-Kenneally, J., and Mlodzik, M. (2002). The atypical cadherin Flamingo links Frizzled and Notch signaling in planar polarity establishment in the *Drosophila* eye. Dev. Cell *2*, 655–666.
9. Adler, P.N. (2002). Planar signaling and morphogenesis in *Drosophila*. Dev. Cell *2*, 525–535.
10. Clandinin, T.R., and Zipursky, S.L. (2000). Afferent growth cone interactions control synaptic specificity in the *Drosophila* visual system. Neuron *28*, 427–436.
11. Lee, T., and Luo, L. (1999). Mosaic analysis with a repressible neurotechnique cell marker for studies of gene function in neuronal morphogenesis. Neuron *22*, 451–461.
12. Ashley, J.A., and Katz, F.N. (1994). Competition and position-dependent targeting in the development of the *Drosophila* R7 visual projections. Development *120*, 1537–1547.
13. Newsome, T.P., Schmidt, S., Dietzl, G., Keleman, K., Åsling, B., Debant, A., and Dickson, B.J. (2000). Trio combines with Dock to regulate Pak activity during photoreceptor axon pathfinding in *Drosophila*. Cell *101*, 283–294.
14. Rajagopalan, S., Vivancos, V., Nicolas, E., and Dickson, B.J. (2000). Selecting a longitudinal pathway: Robo receptors specify the lateral position of axons in the *Drosophila* CNS. Cell *103*, 1033–1045.
15. Granderath, S., Bunse, I., and Klambt, C. (2000). *gcm* and *pointed* synergistically control glial transcription of the *Drosophila* gene *loco*. Mech. Dev. *91*, 197–208.
16. Poeck, B., Fischer, S., Gunning, D., Zipursky, S.L., and Salecker, I. (2001). Glial cells mediate target layer selection of retinal axons in the developing visual system of *Drosophila*. Neuron *29*, 99–113.
17. Brown, A., Yates, P.A., Burrola, P., Ortuno, D., Vaidya, A., Jessell, T.M., Pfaff, S.L., O'Leary, D.D., and Lemke, G. (2000). Topographic mapping from the retina to the midbrain is controlled by relative but not absolute levels of EphA receptor signaling. Cell *102*, 77–88.
18. Feldheim, D.A., Kim, Y.I., Bergemann, A.D., Frisen, J., Barbacid, M., and Flanagan, J.G. (2000). Genetic analysis of ephrin-A2 and ephrin-A5 shows their requirement in multiple aspects of retinocollicular mapping. Neuron *25*, 563–574.
19. Formstone, C.J., and Little, P.F. (2001). The flamingo-related mouse Celsr family (Celsr1–3) genes exhibit distinct patterns of expression during embryonic development. Mech. Dev. *109*, 91–94.
20. Tissir, F., De-Backer, O., Goffinet, A.M., and Lambert de Rouvroit, C. (2002). Developmental expression profiles of Celsr (Flamingo) genes in the mouse. Mech. Dev. *112*, 157–160.
21. Shima, Y., Copeland, N.G., Gilbert, D.J., Jenkins, N.A., Chisaka, O., Takeichi, M., and Uemura, T. (2002). Differential expression of the seven-pass transmembrane cadherin genes Celsr1–3 and distribution of the Celsr2 protein during mouse development. Dev. Dyn. *223*, 321–332.
22. Clandinin, T.R., Lee, C.-H., Herman, T., Lee, R.C., Yang, A.Y., Ovasapyan, S., and Zipursky, S.L. (2001). *Drosophila* LAR regulates R1–R6 and R7 target specificity in the visual system. Neuron *32*, 237–248.
23. Maurel-Zaffran, C., Suzuki, T., Gahmon, G., Treisman, J.E., and Dickson, B.J. (2001). Cell-autonomous and -nonautonomous functions of LAR in R7 photoreceptor axon targeting. Neuron *32*, 225–235.

Note Added in Proof

Lee and colleagues have also recently noted a requirement for Fmi in R8 target selection and have also documented a later function for Fmi in R1–R6 interactions within the lamina. These results can be found in: Lee, R.C., Clandinin, T.R., Lee, C.-H., Chen, P.-L., Meinertzhagen, I.A., and Zipursky, S.L. (2003). The protocadherin Flamingo mediates growth cone interactions essential for target selection in the *Drosophila* visual system. Nat. Neurosci., in press.